Near-Rectilinear Halo Orbit Surveillance using Cislunar Periodic Orbits

Adam P. Wilmer and Robert A. Bettinger
Air Force Institute of Technology, Wright-Patterson Air Force Base, OH

ABSTRACT

Cislunar space is anticipated to become increasingly congested in the coming decades with both nations and private companies building up infrastructure to support missions to the Moon and Mars. With this anticipated increase in space traffic, it is paramount to conduct space surveillance, commonly referred to as Space Situational/Domain Awareness (SSA/SDA), missions in such a way as to encapsulate the entirety of the Earth-Moon system. Performing SSA/SDA utilizing classical ground- and/or near Earth space-based sensors becomes increasingly challenging when applied to the cislunar orbit regime. Therefore, orbits which reside in cislunar space such as cislunar periodic orbits (CPOs) provide an elegant means to fill the observational capability gaps which exist in current near-Earth sensors. This work seeks to compare the effectiveness between a touring class of CPOs, herein referred to as "touring" CPOs and L1/L2 halo orbits in a sample surveillance mission. Specifically, these orbits will be evaluated on their ability to detect and track satellites in a Near Rectilinear Halo Orbit (NRHO) trajectory, such as one intended for NASA's Lunar Gateway that aims to support colonization efforts on the lunar surface for future ventures to Mars. Visual magnitude is used in determining if a target satellite is visible. Notional space-to-space sensors will be used to determine limitations of orbit geometry for the SDA mission as a function of sensor range, capability, and Sun/Earth/Moon exclusion angles. Simulations will consist of 12 sensor satellites in either a touring CPO or an L1/L2 halo orbit, depending on the scenario. These sensor satellites will be monitoring two target satellites in the NRHO. Results show the halo orbits to be more effective than the touring CPOs at NRHO surveillance, with the L1 halo orbit hosting a visual of the Target for an average of 99.28% of the 30 day simulation. This is a result of the conclusion that closeness to the target of interest is one of the most influential factors for successful space surveillance missions.

1. INTRODUCTION

Cislunar[1] space is progressively gaining attention for the opportunities it holds to advance societies. There are many initiatives for technological advances in astrodynamical sciences due to concerns related to the environment or national security, to name a few. For mankind, this is a race to become a multi-planetary species; for nations, this is a race to hold the strategic high ground. Both of these goals requires the formation of missions within the cislunar environment. Specifically, a principal mission within this environment will be monitoring and tracking spacecraft within the cislunar zone. Recently, Vendl [10] has studied periodic orbits for their ability to detect and track objects within cislunar space. Touring Cislunar periodic orbits (CPOs) have been extensively studied by Wilmer [12, 13, 14] for their effectiveness in surveillance type missions commonly referred to as space domain awareness (SDA) mission sets. The allure of touring CPOs is that they provide mission-related benefits in terms of their ability to traverse wide expanses of cislunar space capturing multiple different viewing angles of targets. Touring CPOs are also designed to repeatedly traverse a given region of cislunar space, potentially allowing for a lower propellant expenditure than typical non-periodic cislunar trajectories. However, L1/L2 halo orbits are also designed to repeatedly traverse a region of cislunar space, namely about the L1 and L2 Lagrange points. Therefore, an interesting study, and one which this work seeks to complete, is to compare the effectiveness of touring CPOs with halo orbits on surveilling a Near-Rectilinear Halo Orbit (NRHO).

As part of the ongoing Artemis Program, the National Aeronautics and Space Administration (NASA) has plans for a Gateway lunar orbiter which will act as an outpost providing vital support for a long-term human return to the Moon, as well as a staging point for deep space exploration [1]. The Gateway is planned to be in a 7-day NRHO with a close approach to the Moon. This work acts to provide orbits which have the capability for continued surveillance of

[1]The term "cislunar" refers to the spherical volume of space extending from geosynchronous Earth orbit to and including the Moon's orbit and the Earth-Moon Lagrange points.

such a NRHO. This research will rely on the use of the circular restricted three-body problem (CR3BP). Simulations are performed using notional space-to-space sensors to determine limitations of orbit geometry for the surveillance mission as a function of sensor range and Sun/Earth/Moon exclusion angles. Simulations will consist of 12 sensor satellites in either a touring CPO or a halo orbit about the L1 or L2 Lagrange point, depending on the scenario. These sensor satellites will be monitoring two target satellites in the NRHO. Touring CPOs and/or halo orbits are theorized to be a solution to the problem of detecting and tracking resident space objects within the cislunar domain; thus, this study will develop further understanding of the types of orbits needed for cislunar surveillance.

2. BACKGROUND

For nearly 50 years following the start of the first Space Age in the mid-twentieth century, space represented a supporting function to wider terrestrial conflict – either on land, at sea, or in the air. Space became the "ultimate high ground," as first described by then-USAF chief of staff General Charles Gabriel in 1982, which enabled the introduction of game-changing technologies in the form of persistent overhead surveillance, communication beyond the line-of-sight, and precision navigation and timing that would spur a revolution in U.S. military strategy and operational art in the latter twentieth and early twenty-first centuries [7]. Against this backdrop of space access and utilization, a new mission emerged in the 1960s: early warning and space object tracking and characterization. The proto-form of what would become known as "space situational awareness" (SSA) arose due to the need to differentiate between non-hostile resident space objects (e.g., friendly satellites and debris) and ballistic missile nuclear payloads [11]. The SSA mission grew to encompass four functions: search, detect, track, and characterization. Once a space object is characterized and its position and velocity is known for predictive tracking, then the object is catalogued. At its heart, the SSA mission became one of space traffic management, with ground- and space-based sensors constantly updating and refining the space object catalog in order to de-conflict orbits and generate collision avoidance warnings [2].

Just as the U.S. Air Force (USAF) was created out of the need for service dedicated to attaining and projecting air power in the wake of World War II based on the growing role of the air domain in military and national security operations, the U.S. Space Force (USSF) has emerged as an independent service due to the need to attain and maintain national power and superiority in space – a domain which is now irrevocably linked to U.S. sovereignty and economic power. Until the start of the 2010s, there was general hesitancy to refer to space as a "warfighting domain"; however, the patent realization of space as a domain that is congested, contested, and competitive has prompted an evolution in how space is viewed and framed from a national security perspective [4]. While SSA remains a consistent term used in civilian space flight, the general SSA mission has become a subset of a wider mission set for the Department of Defense – SDA. In a memorandum released to the then-Air Force Space Command in 2019, Major General John Shaw discussed the formal shift from SSA to SDA within the Department of the Air Force, and stated that "the implication of space as a warfighting domain demands we shift our focus beyond the Space Situational Awareness mindset of a benign environment to achieve a more effective and comprehensive SDA" [4]. The document *Spacepower: Doctrine for Space Forces* outlines that SDA "leverages the unique subset of intelligence, surveillance, reconnaissance, environmental monitoring, and data sharing arrangements that provide operators and decision makers with a timely depiction of all factors and actors - including friendly, adversary, and third party - impacting domain operations" [9].

3. METHODOLOGY

3.1 Circular Restricted Three-Body Problem

The CR3BP is often used when modeling the trajectory of spacecraft past GEO orbit. In this dynamical model, the Moon is orbiting the Earth in a perfectly circular orbit. Both the mass of the Earth and Moon influence the motion of the satellite, which is of an assumed negligible mass. This system is often viewed with respect to a synodic reference frame as shown with respect to the inertial reference frame in Fig. 1:

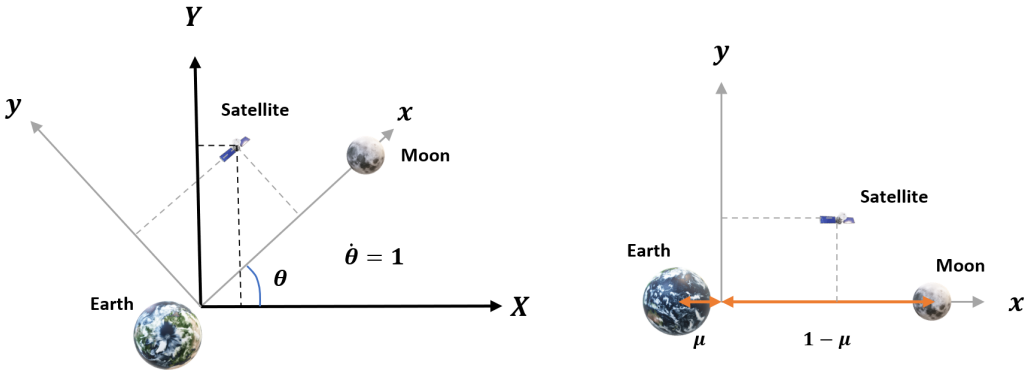

Fig. 1: CR3BP Inertial Reference frame (X,Y) and Synodic Reference Frame (x,y)

In the synodic reference frame the Earth and Moon remain on the x-axis at fixed, non-dimensional distances $-\mu$ and $1-\mu$ respectively. In this analysis, the non-dimensional mass parameter, μ, is equal to 0.012150584673414. The non-dimensional equations of motion are shown in Eq. (1) below:

$$\begin{aligned} \ddot{x} &= x + 2\dot{y} - \frac{(1-\mu)(x+\mu)}{r_{sat/e}^3} - \frac{\mu(x-1+\mu)}{r_{sat/m}^3} \\ \ddot{y} &= y - 2\dot{x} - \frac{(1-\mu)y}{r_{sat/e}^3} - \frac{\mu y}{r_{sat/m}^3} \\ \ddot{z} &= -\frac{(1-\mu)z}{r_{sat/e}^3} - \frac{\mu z}{r_{sat/m}^3} \end{aligned} \tag{1}$$

where the scalar distance of the satellite (*sat*) with respect to the Earth and Moon in the synodic reference frame is written as Eqs. (2) and (3), respectively:

$$r_{sat/e}^2 = (x+\mu)^2 + y^2 + z^2 \tag{2}$$

$$r_{sat/m}^2 = (x-1+\mu)^2 + y^2 + z^2 \tag{3}$$

The variables for distance, time, and mass were non-dimensionalized according to the characteristic quantities given in Table 1. The DU is equal to the distance between the Earth and Moon, the TU is equal to the period of the system divided by a non-dimensional period equal to 2π (i.e. $TU = \frac{P_d}{2\pi}$), and the MU is equal to the sum of the Earth and Moon masses (i.e. $MU = m_e + m_m$). The DU, TU, and MU used in this analysis are provided in Table 1 below:

Table 1: CR3BP Characteristic Quantities

Parameter	Value
Distance Unit (DU)	390,877.4158212686 km
Time Unit (TU)	4.4527 days
Mass Unit (MU)	6.0459×10^{24} kg

Constants used in the CR3BP analysis are shown in Table 2:

Table 2: CR3BP Constants

Parameter	Value
G	$6.674 \times 10^{-20} \frac{Nkm^3}{kg^2}$
m_e	5.9724×10^{24} kg
m_m	7.346×10^{22} kg

3.2 Space Domain Awareness

To determine if the Target satellites in the Lyapunov orbit are visible, visual magnitude (M_v) of the vehicles is calculated. The first step in calculating visual magnitude is to determine the phase (or Sun) angle at every point in time. The phase angle is calculated from Eq. (4):

$$\phi = \arccos\left(\frac{\vec{r}_{Tar/sat} \cdot \vec{r}_{Tar/S}}{r_{Tar/sat} r_{Tar/S}}\right) \tag{4}$$

where $\vec{r}_{Tar/sat}$ is the vector position of the target with respect to the sensor bearing satellite, and $\vec{r}_{Tar/S}$ is the vector position of the target with respect to the Sun. In this analysis, the target is modeled as a sphere; therefore, the phase function, Ψ, becomes:

$$\Psi = \frac{2}{3}\frac{C_d}{\pi}(\sin\phi + (\pi - \phi)\cos\phi) \tag{5}$$

where C_d is the coefficient of diffuse reflection which is a function of the mean wavelength. The visual magnitude, M_v, is then calculated by:

$$M_v = -26.8 - 2.5\log_{10}\left(\frac{A}{r_{Tar/sat}^2}\Psi\right) \tag{6}$$

where A is the surface area of the Target. The visual magnitude is, counterintuitively, measured on a logarithmic scale in which lower numbers indicate brighter objects. For comparison, Table 3 lists common visual magnitudes.

Table 3: Common Visual Magnitudes [8]

Object	M_v
Sun from Earth	-26.8
Full Moon from Earth	-12.5
Jupiter at brightest from Earth	-2.7
Polaris from Earth	1.99
Naked Eye Limit Ability	6.0
Pluto from Earth	15.1
Hubble Space Telescope Ability	31

For this analysis, a Target is considered visible when it has a visual magnitude of $M_v \leq 18.5$. Constants used in the SDA analysis were area of the Target, A, and coefficient of diffuse reflection, C_d which were 2.25 m^2 and 0.86, respectively. It is critical to note that A is converted to kilometers before calculating M_v to match units of r^2.

Exclusion angles are also considered in this analysis, which are the angles between the satellite-Target and satellite-gravitational body. When the angle between the satellite-Target and satellite-gravitational body vectors are less than these exclusion angles, the target is assumed to be imperceptible due to the Sun's reflection onto the respective gravitational body. Table 4 shows the sun exclusion angles used:

Table 4: Exclusion Angles

Object	Value	M_v
Sun	30°	35
Earth	15°	35
Moon	6°	35

For graphical purposes, high M_v values are assigned to angles which are less than the exclusion angle as shown in Table 4. For instance, a M_v value of 35 would correspond to a scenario in which the Target is imperceptible due to either the Sun, Earth, or Moon's exclusion angle.

4. ANALYSIS AND RESULTS

4.1 Sensor and Target Orbits

In performing the SDA simulations, Systems Tool Kit (STK) was utilized to model the sensors and CR3BP dynamics [6]. SDA effectiveness is determined by the percentage of time with which a sensor bearing satellite is able to have a visual site of the Target. The initial conditions of the touring CPOs used in this work were obtained through the works of Wilmer [12, 13] who used a μ value of 0.012150584673414. The initial conditions of these orbits may be seen in Table 5:

Table 5: Generated Touring Cislunar Periodic Orbit Initial Conditions in Analysis

Touring CPO	x_0 (DU)	$\dot{y}_0$ (DU/TU)	T_0 (TU)
1	1.2	-1.05	6.193
2	0.82	0.6558356	11.45
3	1.15	-0.5724	30.819

The initial conditions of the halo orbit was also obtained through the works of Wilmer [12, 13] who followed a method laid out by Grebow [5] in which the bifurcation with the planar Lyapunov orbits was used as the starting point for forming halo orbits. The initial conditions of the halo orbits used in this analysis is shown in Table 6:

Table 6: Halo Orbit Initial Conditions

Halo Orbit	x_0 (DU)	z_0 (DU)	$\dot{y}_0$ (DU/TU)	T_0 (TU)
1 (L1)	0.830970	0.120	0.234856	2.785808
2 (L2)	1.178242	0.05	-0.168829	3.394850

The initial conditions for the NRHO are obtained through the work of Bucchioni and Innocenti [3] and adjusted to fit a standardized non-dimensional mass parameter. The adjusted initial conditions are shown in Table 7:

Table 7: Target NRHO Initial Conditions

Target Orbit	x_0 (DU)	z_0 (DU)	$\dot{y}_0$ (DU/TU)	T_0 (TU)
1	1.02950089	-0.1868081	-0.11898	1.609

The orbits with initial conditions shown in Tables 5, 6, and 3 periodic for at least two full repeating periods where no propellant would be required in the CR3BP. This was to allow for the scenario to play out in STK without risk of divergent trajectories. Plotting the initial conditions from Tables 5 and 6 provides the orbits in Fig. 2. Plotting the initial conditions from Table 3 provides the orbit shown in Fig. 3.

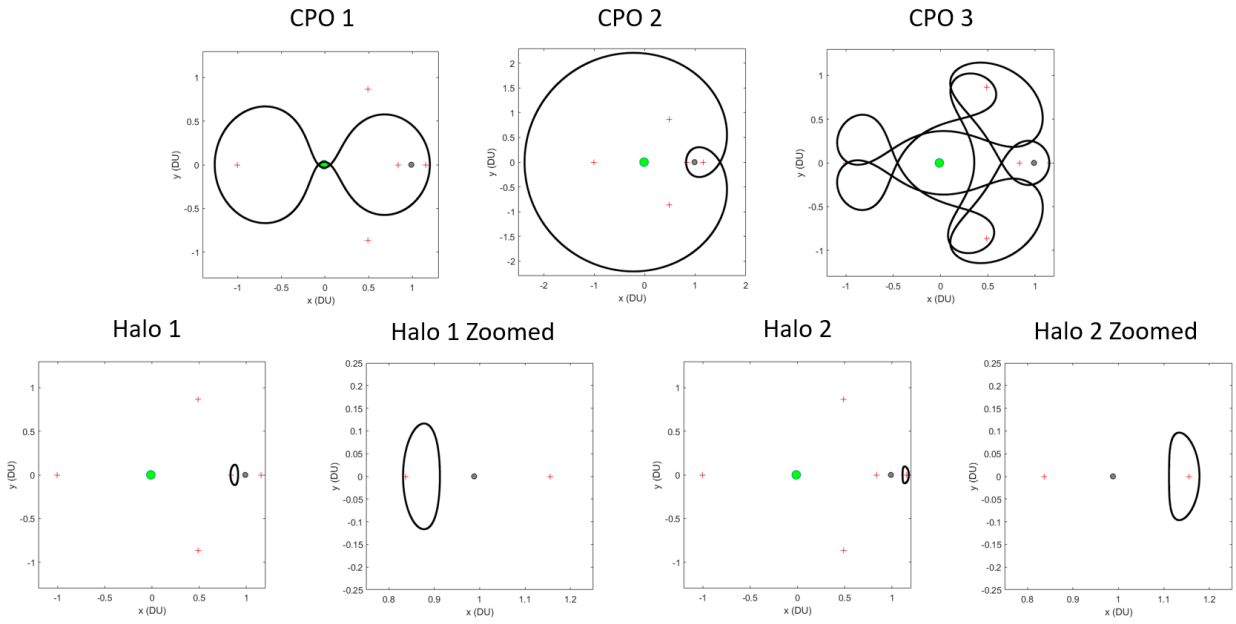

Fig. 2: Sensor Bearing Orbits [12]

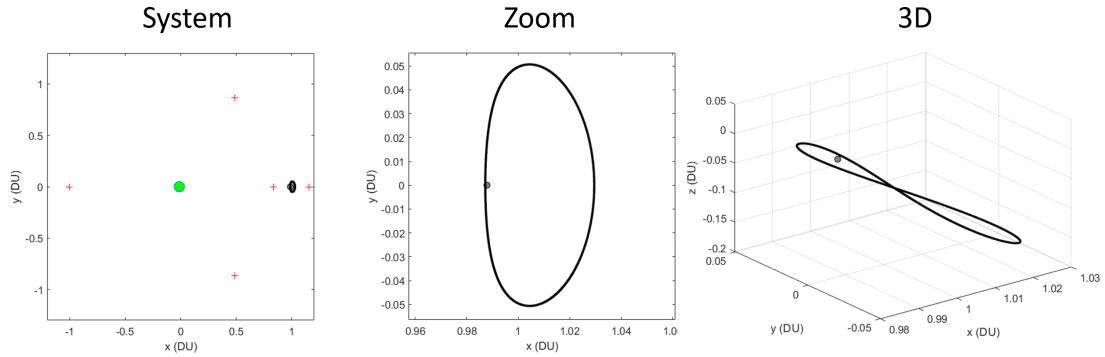

Fig. 3: Target NRHO

CPO 1 hosts the shortest period of the touring CPOs analyzed. This is beneficial in potentially reducing the total number of satellites needed to perform a mission. CPO 2 hosts the second shortest period of the touring CPOs. CPO 2 has a loop about the Moon which Compared to Orbit 1, Orbit 2 has an additional loop on the opposite side of the Earth with respect to the Moon. CPO 3 hosts the longest period and while it does have the shortest dwell time about the Moon, it offer the longest dwell times about L_4 and L_5. This creates multiple viewing angles of the L_4 and L_5. All touring CPOs analyzed provide some section of their trajectory which features a long dwell time around the Moon, a promising attribute for lunar surveillance as well as L_1 and L_2 surveillance.

With regards to Earth passes, CPO 1 has the closest Earth encounter followed by CPO 3. From there CPO 2 and halo orbit 1 both have the section of their trajectories which is closest to Earth in the realm of the L_1 Lagrange point. Finally, halo orbit 2 has the furthest Earth encounter. As a spacecraft gets closer to Earth, air drag and J2 perturbations become more significant; however, these perturbations are beyond the scope of this research.

4.2 Simulation

In this analysis STK's Astrogator system was used to perform all three simulations. While all orbits were propagated in a Earth-Moon CR3BP model within STK, Sun exclusion angles were also considered with the Sun located by a

realistic ephemeris model which is built into STK. The start date and time for all simulations was 28 Mar 2021 at 1600 UTCG. The vector range data during the simulations was obtained in 15 minute intervals.

An efficient way of comparing the effectiveness of each periodic orbit is to reduce as many differences between the scenarios as possible. In reducing free variables between scenarios, the same number of sensor satellites and Targets were chosen for each periodic orbit scenario. For each scenario, 2 Targets were chosen to be traversing the NRHO with 12 sensor bearing satellites orbiting the sensor orbit. Each scenario was propagated for approximately 30 days (6.7375 TU). Both the sensor satellites and Targets were spaced out evenly in time in their respective orbits such that at the beginning of the scenario there was always one satellite in the orbits initial conditions. A Target was assumed to be viewable if at least one of the twelve sensor bearing satellites was able to view it based on visual magnitude.

4.2.1 Results

After a month of simulation time, the average percentage of time which the sensor bearing satellites were able to view the Targets based on visual magnitude was recorded. The two Target's percentage of viewable time was averaged. To assist with visualizing the scenarios, visual representations have been created for all five scenarios and are shown Figs. 4 and 5:

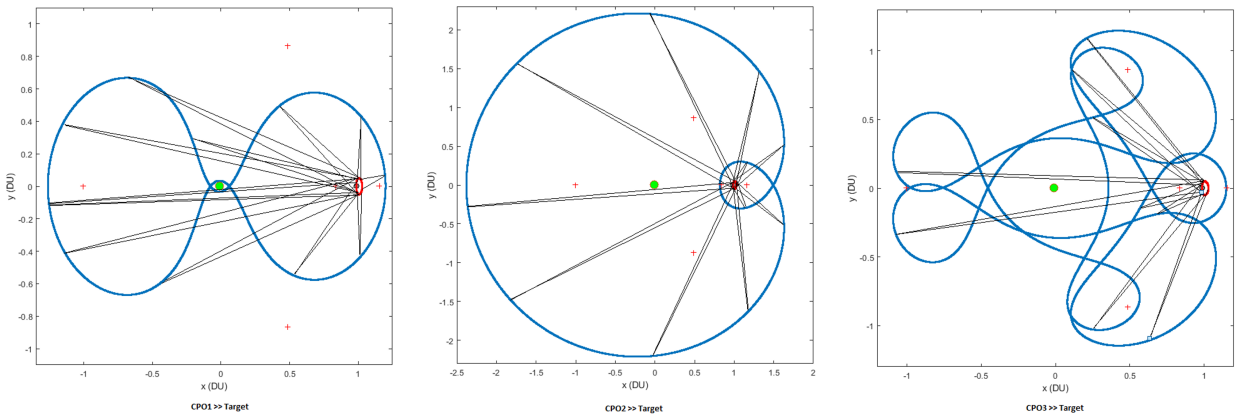

Fig. 4: Surveillance Simulations Utilizing Touring CPOs

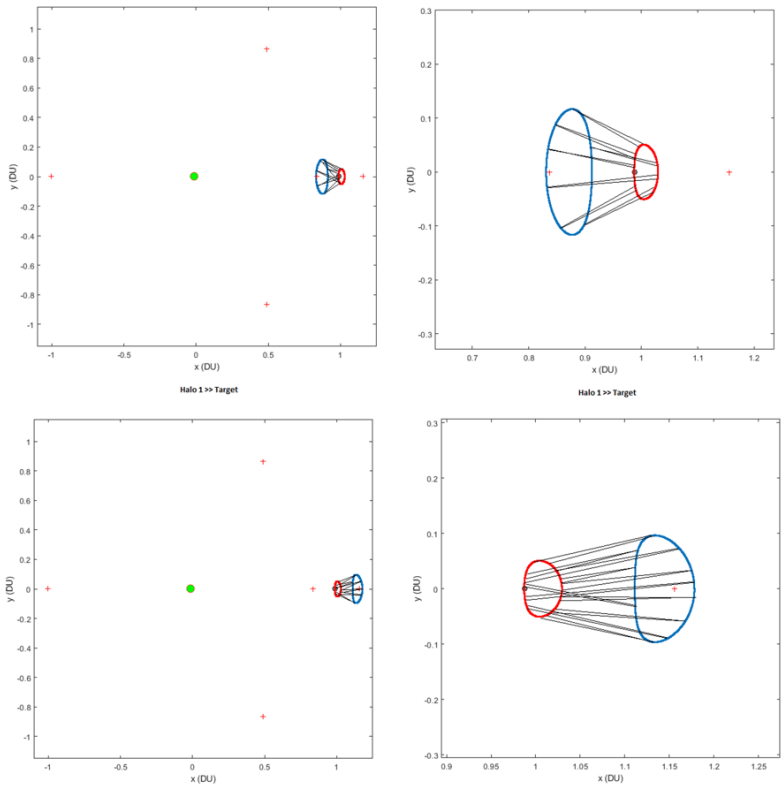

Fig. 5: Surveillance Simulations Utilizing Halo Orbits

As shown in Figs. 4 and 5, the blue orbit depicts the sensor bearing touring CPOs, the red orbit depicts the Target's orbit, and the black lines extending from the green orbit to red orbit depict each sensor's line of sight of the Targets. For Fig. 5, the left subplots represent the halo orbit simulations within the Earth-Moon system while the right subplots represent a zoomed-in view of the same simulation. The results of the simulations are shown in Table 8 with the highest performance (most time, on average, observing the Targets) highlighted green:

Table 8: NRHO Targets Surveillance Results (% Time Visible)

Start Date:	28 Mar 2021		
Orbit	Target 1	Target 2	**Average**
Touring CPO 1	93.48%	92.16%	**92.82%**
Touring CPO 2	96.43%	95.18%	**95.81%**
Touring CPO 3	93.51%	92.51%	**93.01%**
Halo 1 (L1)	99.31%	99.24%	**99.28%**
Halo 2 (L2)	98.85%	98.96%	**98.91%**

The orbits analyzed in this work overall performed exceptionally well in monitoring the NRHO with every case studied hosting an observation of the Target above 90%. As shown in Table 8, the L_1 halo orbit performed the best hosting a 99.28% Target visibility over the 30 day simulation. This means that the Target had a visual magnitude below the threshold value of 18.5 for 99.28 % of the simulation. The L_2 halo orbit was a close second, featuring a 98.96% Target visibility over the 30 day simulation. It is expected that the halo orbits perform better due to their close proximity to the Target NRHO, inducing long dwell times about the Target while minimizing issues with exclusion angles. While the touring CPOs in this case study did not perform as well as the halo orbits, they are theorized to be a highly useful tool in the coming decades for missions to include cislunar surveillance, re-supply, personnel transport, and space-based infrastructure development.

4.3 Recommendations

Halo Orbits 1 and 2 provided similar results for the SDA simulation in terms of how often Targets 1 and 2 were visible. This is intuitively logical as both of these orbits are in close proximity to the NRHO. Both of these orbits were able to view the Targets 3-4% more than the highest performing touring CPO. We recommend that, of the orbits analyzed, the use of the halo orbits over the touring CPOs is most beneficial when conducting surveillance on the case NRHO. However, this is assuming an ideal CR3BP dynamics scenario. In reality, there are many more perturbations which the satellites will experience that will induce chaos and disturb the satellites from their periodic trajectories. Therefore, it is recommended that propellant expenditure (Δv) analysis be performed to determine the feasibility of these orbits.

5. CONCLUSION

Cislunar space is a region of growing interest with nations investing resources to cultivating long presence habitations on the lunar surface. With this increased attention, cislunar orbital pathways must be established and how the spacecraft in these pathways move with respect to one another must be analyzed. With various countries now looking to expand their infrastructure in space, safe space traffic management and surveillance techniques are vital for the continued protection of space-based assets. The orbits analyzed in this work are an ideal candidate for cislunar surveillance missions due to their periodicity, theorized low propellant costs, and ability to traverse a wide expansion of cislunar space (for the CPOs). This work sought to present and compare the effectiveness of three different CPOs and two halo orbits for their ability to conduct continued surveillance on a NRHO, an orbit which will be used for NASA's Lunar Gateway orbiter. Each sensor orbit consisted of 12 sensor-bearing satellites evenly spaced in time surveilling two Target satellites in a NRHO. Visibility was determined based on visual magnitude over a 30 day simulation with Sun, Earth, and Moon exclusion angles considered.

Initial results indicated that the L1 halo orbit to be the most effective at monitoring the NRHO, hosting a 99.28% Target visibility over the course of the simulation. Halo orbit 2 performed nearly as well, hosting a 98.96% Target visibility over the course of the simulation. Halo orbit 1 and 2 both have the longest dwell times (per period) near the Moon than all of the sensor bearing orbits analyzed, thus, it is expected that they would perform the best at surveilling the Target NRHO (recall that visual magnitude is a function of range). In terms of CPO performance, CPO 2 had the highest percentage of time viewing the Target NRHO. This is due to its orbital geometry which consists of a loop around the Moon, capturing many different viewing angles of the Target NRHO. The results of this work show promise for exploiting L_1 and L_2 halo orbits for future NRHO surveillance missions. Additionally, while the CPOs were shown to have slightly lower effectiveness at monitoring the Target NRHO, they may prove beneficial at monitoring other regions of cislunar space or for other missions such as re-supply, personnel transport and/or cargo transport. Future work will aim to analyze CPO feasibility for such mission sets.

6. REFERENCES

[1] National Aeronautics and Space Administration. Gateway. https://www.nasa.gov/gateway/overview, 2022.

[2] Mark A. Baird. Maintaining space situational awareness and taking it to the next level. *Air and Space Power Journal*, 27, 2013.

[3] Giordana Bucchioni and Mario Innocenti. Phasing maneuver analysis from a low lunar orbit to a near rectilinear halo orbit, aerospace. *Aerospace*, 2021.

[4] Sandra Erwin. Air force: Ssa is no more; it's 'space domain awareness'. *Spacenews*, 2019.

[5] Daniel J. Grebow. Generating periodic orbits in the circular restricted three-body problem with applications to lunar south pole coverage. 2006.

[6] Systems Tool Kit. Astrogator: Circular restricted three-body problem (cr3bp) configuration. https://help.agi.com/stk/index.htmtraining/Astro$_C$*R*3*BP.htm*, 2021.

[7] Benjamin S. Lambeth. Mastering the ultimate high ground: Next steps in the military uses of space. *Rand*, page 23, 2003.

[8] Michael A. Seeds and Dana E. Backman. *The Solar System*, volume 7. CENGAGE Learning, 1997.

[9] USSF. Spacepower. *Space Capstone Publication*, page 38, 2020.

[10] Jacob K. Vendl and Marcus J. Holzinger. Cislunar periodic orbit analysis for persistent space object detection capability. *Journal of Spacecraft and Rockets*, 2021.

[11] Brian Weeden, Paul Cefola, and Jaganath Sankaran. Global space situational awareness sensors. *Presented at the Advanced Maui Optical and Space Surveillance Technologies Conference*, 2010.

[12] Adam P. Wilmer. Space domain awareness assessment of cislunar periodic orbits for lagrange point surveillance. Master's thesis, Air Force Institute of Technology, 2021.

[13] Adam P. Wilmer, Robert A. Bettinger, and Bryan D. Little. Cislunar periodic orbit constellation assessment for space domain awareness of l1 and l2 halo orbits. *Proceedings from AIAA ASCEND Conference*, 2021.

[14] Adam P. Wilmer, Robert A. Bettinger, and Bryan D. Little. Preliminary viability assessment of cislunar periodic orbits for space domain awareness. *2021 Advanced Maui Optical and Space Surveillance Technologies Conference (AMOS)*, 2021.